Appl Phys B (2012) 106:57–62
DOI 10.1007/s00340-011-4669-y

Applied Physics B
Lasers and Optics

AlGaInAs multiple-quantum-well 1.2-μm semiconductor laser in-well pumped by an Yb-doped pulsed fiber amplifier

Y.-F. Chen · Y.C. Lee · S.C. Huang · K.F. Huang · Y.F. Chen

Received: 21 March 2011 / Revised version: 17 June 2011 / Published online: 30 July 2011

Abstract An AlGaInAs multiple quantum well structure is reported as an effective gain medium of the in-well pumped high-peak-power semiconductor disk laser at 1.2 μm. We use an Yb-doped pulsed fiber amplifier as the pump source to effectively optimize the output characteristics. The maximum average output power of 1.28 W and peak output power of 0.76 kW is obtained at 1225 nm lasing wavelength under 60 kHz pump repetition rate and 28 ns pump pulse width.

1 Introduction

High-peak-power all-solid-state lasers operating at 1.14–1.25 μm are desirable for producing yellow-orange lights for many applications such as astronomy community, biomedical optics, and laser absorption spectroscopy [1–3]. Light sources in this spectral range could be realized by Raman-shifted Nd- (Yb-) doped solid-state lasers or Yb- (Bi-) doped fiber lasers [4–6]. However, the performance of solid-state lasers is limited by the discrete energy level of the doped ions. Alternatively, optically pumped semiconductor lasers (OPSLs) have been developed to provide flexible choice of emission wavelength via bandgap engineering [7, 8]. OPSLs also offer a variety of advantages like broad gain curves and a low-divergence, circular, and high quality nearly-diffraction-limited output beam [7–9]. So far, the lasers based on the quantum confined structure with GaAs material systems including InGaAs/GaAs and GaInNAs/GaAs have been demonstrated in the 1.14–1.25 μm spectral range under continuous-wave operation [10–13]. However, these lasers are pumped by exciting the electrons from the barrier region and the quantum defect between pump and lasing photons leads to a large amount of heat. Recently, a novel method based on the in-well pumping scheme has been demonstrated to reduce the heat effectively [14, 15]. For the in-well pumping scheme, the electrons are directly excited from the ground state to the excited state in the quantum-well (QW) region. As a result, the thermal load is reduced by lowering the quantum defect. However, OPSLs at 1.14–1.25 μm based on the in-well pumping scheme have not been explored until now.

The quaternary alloys lattice matched to InP such as AlGaInAs and InGaAsP are employed in the semiconductor lasers in the near-infrared (NIR) spectral region. The AlGaInAs systems have been verified to have higher conduction band offset and better carrier confinement than the InGaAsP systems. Several high-peak-power AlGaInAs semiconductor disk lasers have been demonstrated in the NIR region driven by the actively Q-switched (AQS) solid-state lasers [16–18]. However, the pulse width of conventional AQS solid-state lasers depends on the pulse repetition rate and the average pump power. Consequently, it is difficult to optimize the output performance of the semiconductor disk lasers. Therefore, a light source with fixed pulse duration under various repetition rates can be a more suitable pump source for optimizing the performance of OPSLs. High-power pulsed fiber amplifiers are a light source to satisfy this requirement [19].

In this work, we report on a high-peak-power AlGaInAs multiple-quantum-well (MQW) semiconductor laser grown on a Fe-doped InP transparent substrate and pumped by a 1.06 μm Yb-doped pulsed fiber amplifier. With in-well pumping, the thermal and roll-over effect could be reduced

Y.-F. Chen · Y.C. Lee · S.C. Huang · K.F. Huang · Y.F. Chen (✉)
Department of Electrophysics, National Chiao Tung University, Hsinchu, Taiwan
e-mail: yfchen@cc.nctu.edu.tw
Fax: +886-35-725230

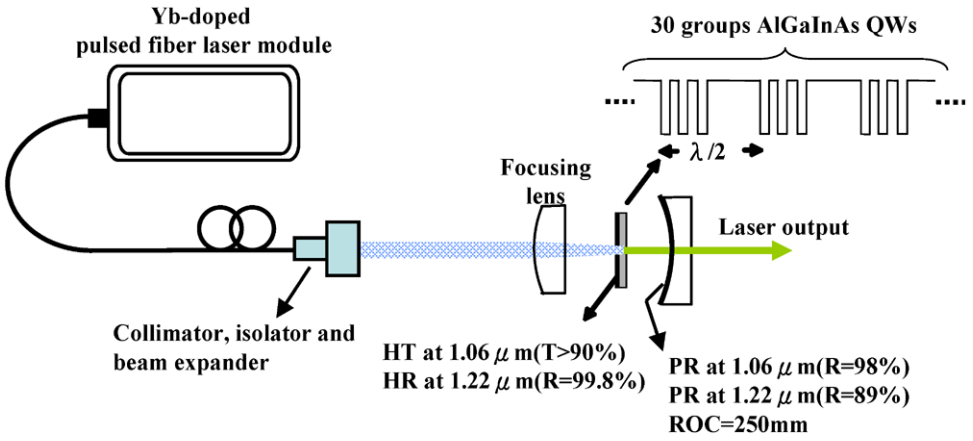

Fig. 1 Experimental setup of AlGaInAs/InP semiconductor disk laser at 1.2 μm pumped by a 1.06 μm Yb-doped pulsed fiber amplifier in the single chip scheme

by lowering the quantum defect. We obtained an average output power of 810 mW at 1225 nm with slope efficiency up to 46.7% to the average absorbed power in the single-chip scheme. The pump conditions of 60 kHz pulse repetition rate and 28 ns pulse width are used. To increase the average absorbed power, the double-chips scheme is used under the same pump conditions. The maximum average output power could be scaled up to 1.28 W with slope efficiency of 37.5% at 1225 nm lasing wavelength. The maximum peak output power of 0.76 kW is obtained with 2.37 kW peak pump power.

2 Device structure and experimental setup

Figure 1 shows the experimental configuration of the AlGaInAs MQW 1.2 μm semiconductor disk laser pumped by a SPI 1.06 μm Yb-doped master oscillator fiber amplifier. This pump source provides 9–200 ns pulse with repetition rate ranged from 10–500 kHz. Compared to the AQS solid-state laser, this laser module can provide fixed pulse width of output pulse even when the output power is changed. We controlled pump spot diameter to be about 800 μm to have efficient spatial overlap with the lasing mode. The gain region is composed of an AlGaInAs QW/barrier structure grown on a Fe-doped InP transparent substrate by metalorganic chemical-vapor deposition. It consisted of 30 groups of triple QWs spaced at half-wavelength intervals by AlGaInAs barrier layers as shown in the inset of Fig. 1. This is a resonant-periodic-gain structure that barrier layers are used to locate the quantum well region at the antinode of the lasing field standing wave. In this structure, the wavelength selection is enhanced [20, 21]. A window layer of InP was deposited on the gain structure to prevent surface recombination and oxidation. In contrast to the conventional barrier pumping scheme, our gain medium is in-well pumped by a 1.06 μm Yb-doped pulsed fiber amplifier. This pumping scheme results in the low absorption (58%) but high conversion efficiency due to the short active region and the small quantum defect, respectively. In our previous work, we have also verified that the in-well pumping scheme has better slope efficiency than the barrier pumping scheme at equivalent absorbed pump power [18].

The InP based systems suffer from the lack of good distributed-Bragg-reflector (DBR) and have been challenging to transfer from edge-emitting lasers to surface-emitting lasers. A number of lattice-matched DBRs such as AlGaInAs/AlInAs, AlGaInAs/InP, GaInAsP/InP, AlGaAsSb/AlAsSb, and AlGaAsSb/InP have been demonstrated [22, 23]. Unfortunately, these DBR systems suffer from the low refractive index contrast, low thermal conductivity or high complexity of growth. Therefore, Fe-doped InP with good transparency in the lasing wavelength is chosen as the substrate system instead of conventional S-doped InP with large absorption in the 1.0–2.0 μm spectral region. As a result, the function of DBRs could be replaced by an external mirror. In this configuration, the problem of fabrication of good DBRs has been resolved and the heat dissipation is improved by reducing the length of thermal conduction.

The laser gain medium is fabricated with dielectric coated mirror on the cap layer served as a front mirror. This forms high transmittance at 1.06 μm ($T > 90\%$) and high reflectance between 1.18–1.25 μm ($R > 99.8\%$) on the entrance face. We use an external mirror with radius of curvature of 250 mm and partial reflectance at 1.22 μm ($R = 89\%$) as output coupler. The overall cavity length is about 3 mm. With this plano-concave linear cavity, we could modulate the laser mode volume to have better efficiency. The gain medium is attached on a cooper heat sink with substrate side and is cooled down by water with temperature controlled to be 15°C.

3 Experimental results and discussion

Figure 2(a) shows the room temperature spontaneous-emission spectrum of AlGaInAs MQW with dielectric

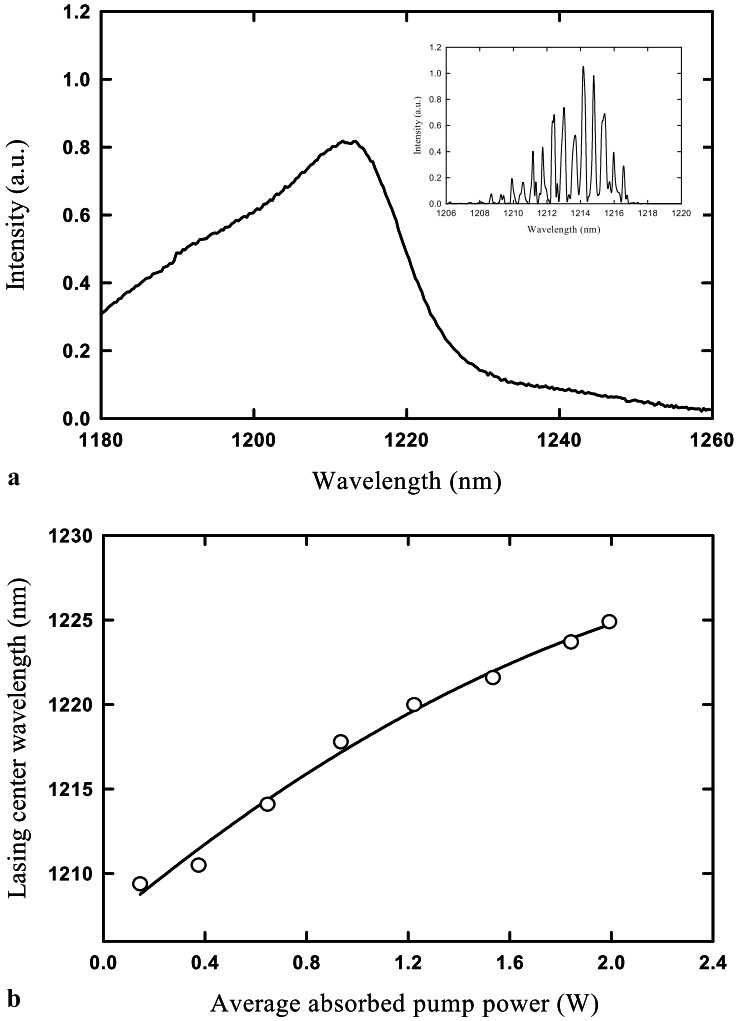

Fig. 2 (**a**) Room temperature surface emitting spontaneous emission spectrum under 60 kHz pump repetition rate and 28 ns pump pulse width at average absorbed power of 0.38 W. *Inset*, the expanded lasing spectrum obtained with 0.85 W average absorbed power under the same pump conditions. (**b**) Redshift of peak lasing wavelength as a function of average absorbed power under 60 kHz pump repetition rate and 28 ns pump pulse width

coated mirror excited by the 1.06 μm Yb-doped pulsed fiber amplifier with average absorbed power of 0.38 W. The pump repetition rate is 60 kHz and the pump pulse width is 28 ns. This surface emitting photoluminescence (PL) spectrum is captured with the pump beam incident on the dielectric coated side, and the emitted light is collected into the multimode fiber on the other side. The spectral information was monitored by an optical spectrum analyzer (Advantest Q8381A) with a diffraction monochromator which can be used for high-speed measurement of pulsed light with a resolution of 0.1 nm. The PL peak is located at 1215 nm. The expanded lasing spectrum is shown in the inset of Fig. 2(a) at the average absorbed power of 0.85 W. The bandwidth of lasing spectrum is about 9 nm, and it comprises dense longitudinal modes due to the multiple interferences between the cavity mirrors. With increasing average pump power, the lasing spectrum will redshift due to the temperature induced shift of cavity resonance and MQW emission peak. In Fig. 2(b), the degree of redshift of peak lasing wavelength is shown as a function of average absorbed power. It will be shifted to 1225 nm at average absorbed power of 2.2 W as the roll-over effect happened.

Figure 3 shows the laser output performances with fixed pump pulse width of 28 ns and different pump repetition rates varied from 40–80 kHz. Under 40 kHz pump repetition rate, the average output power begins to saturate with absorbed power exceeded 2 W, i.e., the maximum allowed pump intensity is approximately 0.35 MW/cm^2. Since the saturation intensity of the MQW absorption was measured to be approximately 0.4 MW/cm^2, the power roll-over phenomenon at 40 kHz was attributed to the pump-saturation effect. On the other hand, the average output power at 80 kHz is also limited when the average absorbed power increased up to 2 W. This is mainly due to the local heating effect which is resulted from the high pump repetition rate. Consequently, the output performance at fixed pump pulse width of 28 ns can be optimized under 60 kHz pump repetition rate. The maximum average output power of 810 mW at 1225 nm is generated by the average absorbed power of 2 W. The slope efficiency to the average absorbed power is calcu-

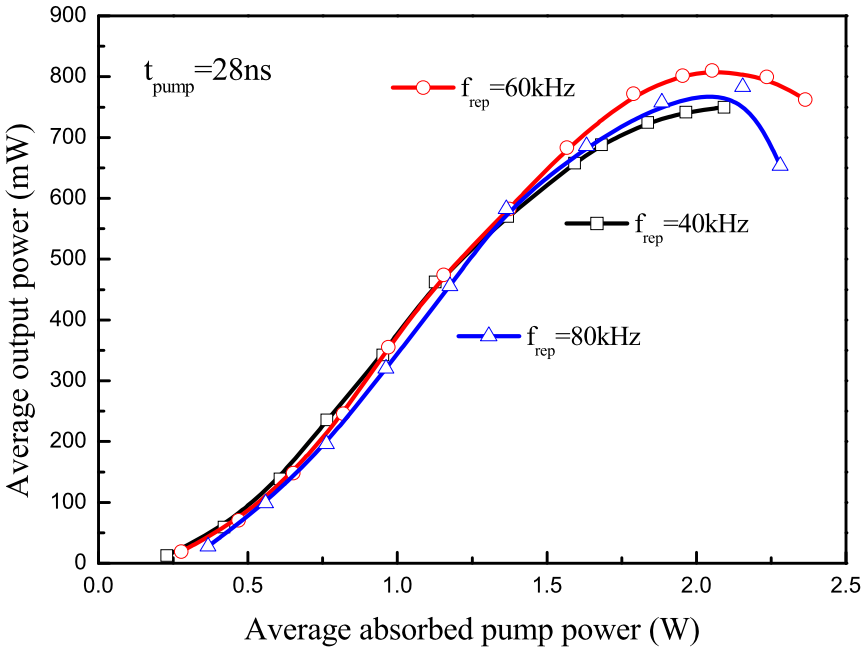

Fig. 3 Laser output performances at fixed pump pulse width of 28 ns and different pump repetition rates ranged from 40–80 kHz

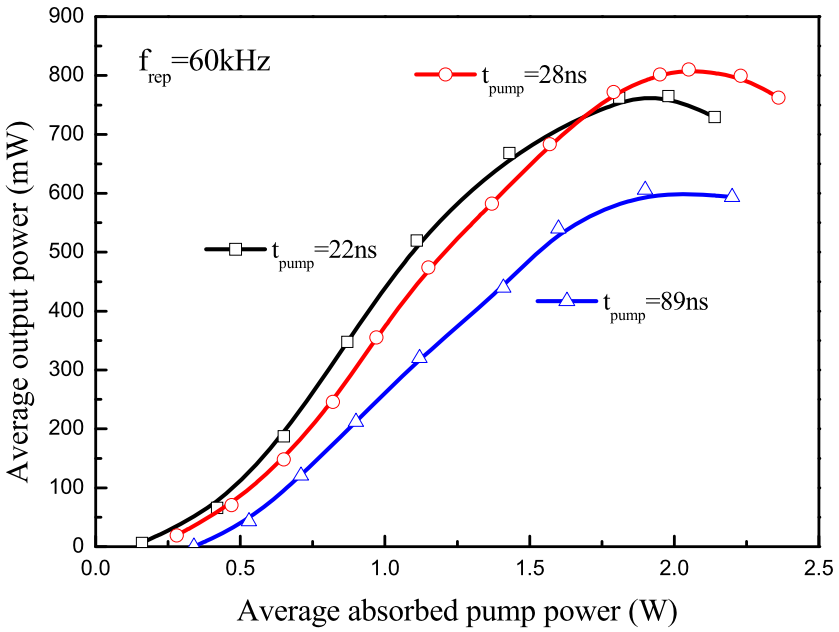

Fig. 4 Laser output performances under 60 kHz pump repetition rate with varied pump pulse width

lated to be 46.7%. The overall beam quality M2 was found to be better than 1.3.

Figure 4 shows the laser output performance with fixed pump repetition rate of 60 kHz and different pump pulse width varied from 22–89 ns. For the given cavity and average absorbed power, the maximum average output power was limited using short pulse width which resulted in the pump-saturation effect [17]. When the pulse duration is long, the roll-over effect appealed due to the thermally induced carrier leakage. As a result, the best performance is obtained under 28 ns pump pulse width. The absorbed saturation intensity of 22 ns and 28 ns pump pulse width is calculated to be 0.3 MW/cm^2 and 0.24 MW/cm^2, respectively. The slightly lower saturation intensity of 28 ns pump pulse width is due to the larger amount of heat. By contrast, the maximum absorbed intensity of 89 ns pump pulse width is 0.07 MW/cm^2. This shows that the roll-over is mainly arisen from the considerable heat production with long pump pulse width. Moreover, the conversion efficiency is strongly affected by the thermal load before roll-over effect happens. Hence, the slope efficiency is higher for lower pump pulse width under low average absorbed power.

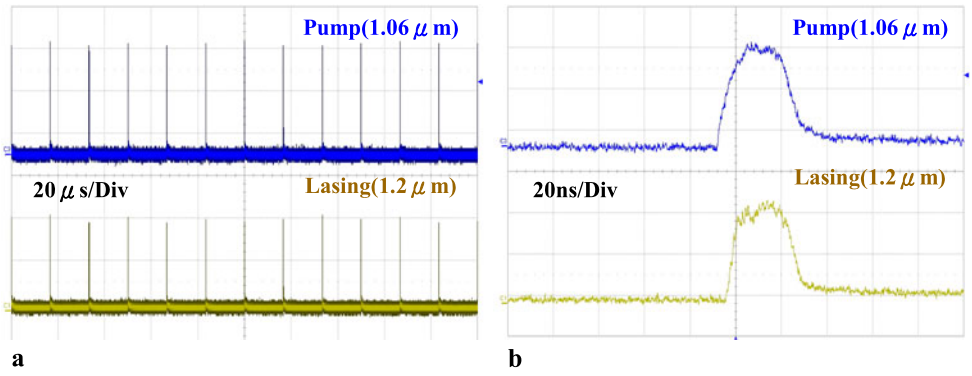

Fig. 5 (**a**) Typical oscilloscope trace of a train of pump and output pulses and (**b**) expanded shapes of a single pulse

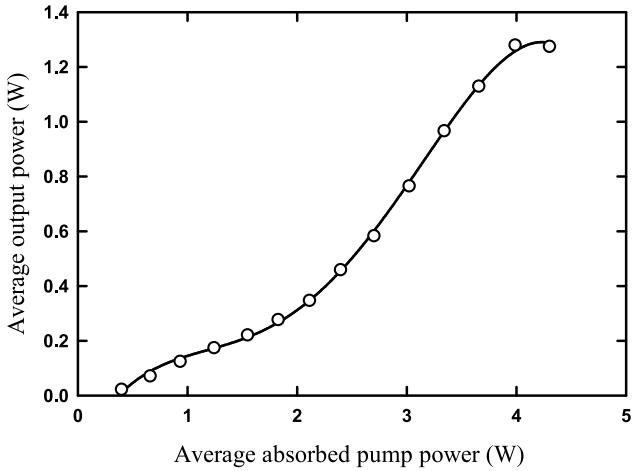

Fig. 6 Output performance with double chips at 60 kHz pump repetition rate and 28 ns pump pulse width

With a LeCrory digital oscilloscope (Wave pro 7100, 10 G samples/s, 1 GHz bandwidth), the typical input and output pulse train as well as the extended pulse shape of single pulse are shown in Fig. 5. It can be seen that the output pulse shape tracked the input pulses with barely delayed turn-on time due to the in-well pump scheme [18]. And the pulse-to-pulse fluctuation was found to be within ±5%, which is mainly attributed to the instability of the pump beam.

To increase the average absorbed power of gain medium without the fabrication of more MQW, we insert another gain chip with the same MQW structure but without the dielectric coating and keep the same experimental setup as shown in Fig. 1. The absorption of double-chips scheme (82%) is 1.41 times higher than the single-chip scheme (58%). The highest average absorbed power is increased to 4 W before the roll-over effect appeared. In this setup, the thermal load is distributed to the two chips. Figure 6 shows the output characteristic of double-chips scheme operated under 60 kHz pump repetition rate and 28 ns pump pulse width. The average output power could be scaled to 1.28 W with 4 W average absorbed power at 1225 nm. Although this method enhanced the absorption and dispersed the generated heat, the asynchronous PL emission due to the inhomogeneous heat distribution and the additional loss make the slope efficiency to be 37.5% which is lower than the single-chip scheme. With this setup, the peak output power is up to 0.76 kW at a peak pump power of 2.37 kW under the same pump conditions.

4 Conclusion

In summary, a high-peak-power semiconductor disk laser at 1.2 μm optically-pumped by a Yb-doped pulsed fiber amplifier has been developed. The gain medium is an AlGaInAs MQW structure grown on a Fe-doped InP substrate by metalorganic chemical-vapor deposition. With in-well pumping, we could reduce the thermal and roll-over effect by lowering the quantum defect. The average output power of 810 mW at 1225 nm lasing wavelength is generated at an average absorbed power of 2 W under 60 kHz pump repetition rate and 28 ns pump pulse width in the single-chip scheme. With the double chips, the average output power could be scaled up to 1.28 W at an average absorbed power of 4 W. The peak output power of 0.76 kW is obtained with 2.37 kW peak pump power.

Acknowledgements The authors gratefully acknowledge various AlGaInAs/InP gain chips from TrueLight Corporation. The authors also thank the National Science Council for their financial support of this research under Contract No. NSC-97-2112-M-009-016-MY3.

References

1. R.Q. Fugate, D.L. Fried, G.A. Ameer, B.R. Boeke, S.L. Browne, P.H. Roberts, R.E. Ruane, G.A. Tyler, L.M. Wopat, Nature **353**, 144 (1991)
2. R.E. Fitzpatrick, Opt. Photonics News **6**, 24 (1995)
3. A.D. Singh, M. Nouri, C.L. Shields, J.A. Shields, N. Perez, Ophthalmology **109**, 1799 (2002)
4. H.M. Pask, J.A. Piper, Opt. Lett. **24**, 1490 (1999)
5. A. Shirakawa, H. Maruyama, K. Ueda, C.B. Olausson, J.K. Lyngsø, J. Broeng, Opt. Express **17**, 447 (2009)

6. E.M. Dianov, A.V. Shubin, M.A. Melkumov, O.I. Medvedkov, I.A. Bufetov, J. Opt. Soc. Am. B **24**, 1749 (2007)
7. A.C. Tropper, H.D. Foreman, A. Garnache, K.G. Wilcox, S.H. Hoogland, J. Phys. D **37**, R75 (2004)
8. L. Fan, M. Fallahi, J.T. Murray, R. Bedford, Y. Kaneda, J. Harder, A.R. Zakharian, J.V. Moloney, S.W. Koch, W. Stolz, Appl. Phys. Lett. **88**, 021105 (2006)
9. M. Kuznetsov, F. Hakimi, R. Sprague, A. Mooradian, IEEE Photonics Technol. Lett. **9**, 1063 (1997)
10. L. Fan, C. Hessenius, M. Fallahi, J. Harder, H. Li, J.V. Moloney, W. Stolz, S.W. Koch, J.T. Murray, R. Bedford, Appl. Phys. Lett. **91**, 131114 (2007)
11. V.-M. Korpijärvi, T. Leinonen, J. Puustinen, A. Härkönen, D. Guina, Opt. Express **18**, 25633 (2010)
12. V.-M. Korpijärvi, M. Guina, J. Puustinen, P. Tuomisto, J. Rautiainen, A. Härkönen, A. Tukiainen, O. Okhotnikov, M. Pessa, J. Cryst. Growth **311**, 1868 (2009)
13. J. Rautiainen, I. Krestnikov, M. Butkus, E.U. Rafailov, O.G. Okhotnikov, Opt. Lett. **35**, 694 (2010)
14. M. Schmid, S. Benchabane, F. Torabi-Goudarzi, R. Abram, A.I. Ferguson, E. Riis, Appl. Phys. Lett. **84**, 4860 (2004)
15. J. Wagner, N. Schulz, M. Rattunde, C. Ritzenthaler, C. Manz, C. Wild, K. Köhler, Phys. Status Solidi **4**, 1594 (2007)
16. K.W. Su, S.C. Huang, A. Li, S.C. Liu, Y.F. Chen, K.F. Huang, Opt. Lett. **31**, 2009 (2006)
17. S.C. Huang, H.L. Chang, K.W. Su, A. Li, S.C. Liu, Y.F. Chen, K.F. Huang, Appl. Phys. B **94**, 483 (2009)
18. H.L. Chang, S.C. Huang, Y.-F. Chen, K.W. Su, Y.F. Chen, K.F. Huang, Opt. Express **17**, 11409 (2009)
19. P. Dupriez, A. Piper, A. Malinowski, J.K. Sahu, M. Ibsen, B.C. Thomsen, Y. Jeong, L.M.B. Hickey, M.N. Zervas, J. Nilsson, D.J. Richardson, IEEE Photonics Technol. Lett. **18**, 1013 (2006)
20. M.Y.A. Raya, S.R.J. Brueck, M. Osinsky, C.F. Schaus, J.G. Mcinery, T.M. Brennan, B.E. Hammons, IEEE J. Quantum Electron. **26**, 1500 (1989)
21. M.Y.A. Raya, S.R.J. Brueck, M.O. Scully, C. Lee, Phys. Rev. A **44**, 4599 (1991)
22. J.H. Biek, I.H. Choi, B. Lee, W.S. Han, H.K. Cho, Appl. Phys. Lett. **75**, 1500 (1999)
23. N. Nishiyama, C. Caneau, B. Hall, G. Guryanov, M.H. Hu, X.S. Liu, M.J. Li, R. Bhat, C.E. Zah, IEEE J. Sel. Top. Quantum Electron. **11**, 990 (2005)